RhoA signaling in cardiomyocytes protects against stress-induced heart failure but facilitates cardiac fibrosis

Published in final edited form as:
Sci Signal. ; 7(348): ra100. doi:10.1126/scisignal.2005262.

RhoA signaling in cardiomyocytes protects against stress-induced heart failure but facilitates cardiac fibrosis

Jessica Lauriol[1], **Kimberly Keith**[1], **Fabrice Jaffré**[1], **Anthony Couvillon**[1,2], **Abdel Saci**[1,3], **Sanjeewa A. Goonasekera**[4], **Jason R. McCarthy**[5], **Chase W. Kessinger**[6], **Jianxun Wang**[1], **Qingen Ke**[1], **Peter M. Kang**[1], **Jeffery D. Molkentin**[4], **Christopher Carpenter**[1,7], and **Maria I. Kontaridis**[1,8,*]

[1]Department of Medicine, Beth Israel Deaconess Medical Center, Boston, MA 02115

[4]Department of Pediatrics, University of Cincinnati, Cincinnati Children's Hospital Medical Center, Howard Hughes Medical Institute, Cincinnati, OH 45229

[5]Center for Systems Biology, Massachusetts General Hospital and Harvard Medical School, Boston, MA 02114

[6]Cardiovascular Research Center, Massachusetts General Hospital and Harvard Medical School, Boston, MA 02114

[8]Department of Biological Chemistry and Molecular Pharmacology, Harvard Medical School, Boston, MA 02115

Abstract

The Ras-related guanosine triphosphatase RhoA mediates pathological cardiac hypertrophy, but also promotes cell survival and is cardioprotective after ischemia/reperfusion injury. To understand how RhoA mediates these opposing roles in the myocardium, we generated mice with a cardiomyocyte-specific deletion of RhoA. Under normal conditions, the hearts from these mice showed functional, structural, and growth parameters similar to control mice. Additionally, the hearts of the cardiomyocyte-specific, RhoA-deficient mice subjected to transverse aortic constriction (TAC)--a procedure that induces pressure overload and, if prolonged, heart failure--exhibited a similar amount of hypertrophy as wild-type mice subjected to TAC. Thus, neither normal cardiac homeostasis nor the initiation of compensatory hypertrophy required RhoA in cardiomyocytes. However, in response to chronic TAC, hearts from mice with cardiomyocyte-specific deletion of RhoA showed greater dilation, with thinner ventricular walls and larger chamber dimensions, and more impaired contractile function than hearts from control mice

[*]Address Correspondence to: Dr. Maria Irene Kontaridis, BIDMC, Department of Medicine, Division of Cardiology, Center for Life Sciences, Room 908, 3 Blackfan Circle, Boston, MA 02115, Tel: 617-735-4248, mkontari@bidmc.harvard.edu.
[2]Current address: Antibody Development, Cell Signaling Technology, Danvers, MA 01923.
[3]Current address: Novartis Institutes for Biomedical Research, Cambridge, MA 02139.
[7]Current address: Oncology Research and Development, Glaxo-Smith Kline, Collegeville, PA 19104.

Author contributions: J.L. performed the majority of the experiments and analyzed the data herein; K.K. conducted the cardiac echo analyses on mice; F.J. conducted the RT-PCR analyses, J.R.M. and C.W.K. conducted fibrosis analysis; A.C., A.S. and C.C generated the RhoA$^{fl/fl}$ mice, S.A and J.D.M. conducted the calcium measure analyses, Q.K. and P.K. conducted the TAC experiments, J.W. provided valuable mechanistic insight; and M.I.K. directed the study, analyzed the data, and wrote the paper with input from all the authors.

Competing interests: The authors declare that they have no competing interests.

subjected to chronic TAC. These effects were associated with aberrant calcium signaling, as well as decreased activity of extracellular signal-regulated kinases 1 and 2 (ERK1/2) and AKT. In addition, hearts from mice with cardiomyocyte-specific RhoA deficiency also showed less fibrosis in response to chronic TAC, with decreased transcriptional activation of genes involved in fibrosis, including myocardin response transcription factor (MRTF) and serum response factor (SRF), suggesting that the fibrotic response to stress in the heart depends on cardiomyocyte-specific RhoA signaling. Our data indicated that RhoA regulates multiple pathways in cardiomyocytes, mediating both cardio-protective (hypertrophy without dilation) and cardio-deleterious effects (fibrosis).

Introduction

Cardiomyocytes undergo remodeling in response to pathological stimuli, such as neurohumoral factors, pressure or volume overload, biomechanical stress, myocarditis, or inherited mutations (1–3). This causes cells to change morphology, increase protein synthesis and reactivate the cardiac fetal gene expression program. While initially compensatory, these changes ultimately prove maladaptive, leading to adverse ventricular remodeling through increased biomechanical stress, loss of contractility and function, and initiation of aberrant signaling processes that eventually cause heart failure. (1, 3). Thus, understanding the cellular signaling events regulating cardiac function may facilitate therapeutic measures to prevent development of cardiac disease.

RhoA belongs to the Rho subfamily of GTP-binding proteins that regulate the actin cytoskeleton. Specifically, RhoA plays a key role in both actin stress fiber formation and focal adhesion complex assembly in fibroblasts (4). Regulation of RhoA occurs at the levels of translocation from cytoplasm to the plasma membrane and GDP/GTP cycling (4, 5). The activation and inactivation of Rho-GTPase is thereby modulated by integrated internal signaling and/or extracellular signaling from G-protein coupled receptors (GPCRs), integrins and growth factor receptors (4, 6).

Once activated, RhoA signals directly to its two downstream effectors, the Rho kinases ROCK-1 and ROCK-2 (Rho-associated coiled-coil protein kinases). In smooth muscle, ROCK-1 phosphorylates the myosin binding subunit of myosin light chain (MLC) phosphatase, resulting in increased myosin phosphorylation and contraction, whereas ROCK-2 activates the LIM domain-containing kinase (LIMK), resulting in actin reorganization through inhibition of the globular G-actin state and depolymerization of filamentous F-actin, to facilitate cellular movement and contraction (7). Principally though, the role for RhoA signaling in smooth muscle is to mediate calcium sensitization and to enhance and sustain contraction, likely through downstream-mediated activation of transcriptional genes, such as the serum response factor (SRF).

In the myocardium, however, the role for RhoA is less defined and apparently dichotomous. Several studies, including investigations in humans, show important pathophysiological roles for RhoA in the cardiovascular system and in disease states such as hypertension, heart failure, stroke, and diabetes (8, 9). In mouse models, aberrant RhoA signaling is associated with *in vivo* pathological hypertrophy (4, 6, 10–14), apoptosis (15) and cardiomyopathy

(16). However, RhoA signaling also promotes cell survival through the regulation of phosphoinositide 3-kinase (PI3K), focal adhesion kinase (FAK), AKT, and phosphatase and tensin homologue (PTEN) (15, 17). Indeed, and as testament to the bi-functional role for RhoA signaling in the heart, chronic administration of the ROCK inhibitors Y-27632 and fasudil prevents cardiac hypertrophy and remodeling (18, 19); however, pharmacological inhibition of ROCK-1 inhibits myocardial fibrosis, not hypertrophy, in response to myocardial infarction and chronic hypertension in a rat model of congestive heart failure (20, 21). *In vivo*, overt overexpression of RhoA leads to dilated cardiomyopathy and heart failure, inducing sinus and atrioventricular nodal dysfunction, severe edema, increased cardiac fibrosis, atrial enlargement, and decreased fractional shortening (13). However, conditional transgenic expression of low amounts of activated RhoA in cardiomyocytes confers protection against ischemia/reperfusion injury *in vivo* and in isolated perfused hearts (22). In addition, treatment of mice with the ROCK inhibitor Y-27632 reduces infarct size and apoptosis following ischemia/reperfusion (23, 24), yet mice deficient in RhoA show increased injury (22). Together, these data delineate different roles for RhoA in the heart; however, the mechanisms by which RhoA regulates cardiac contraction, fibrosis and hypertrophy have not yet been delineated, although similar mechanisms as those observed in smooth muscle cells have been proposed (25).

To directly determine the effects of RhoA specifically in cardiomyocytes and in response to chronic cardiac stress, we generated $RhoA^{fl/fl}$ mice crossed to mice expressing the Cre recombinase under the control of the α myosin heavy chain promoter (α MHC-Cre mice). Our data demonstrate that under these conditions, loss of RhoA in cardiomyocytes leads to decreased contractility, more severe heart failure, and decreased fibrosis, suggesting that RhoA is an integral and nodal enzyme necessary for cardiac function in response to stress in the heart.

Results

Mice with cardiomyocyte-specific deletion of RhoA do not have an overt basal pathological phenotype

We generated a “floxed” allele of *RhoA* ($RhoA^{fl/fl}$) by flanking exon 3 with loxP sites and a Neomycin (Neo) cassette, which was flanked with frt sites. The Neo cassette was removed by crossing mice with flippase-mediated recombination (Frt mice), generating $RhoA^{fl/fl}$ mice that were then crossed to Cre recombinase for tissue specific deletion of RhoA (Supplemental Figure 1A). $RhoA^{fl/fl}$ mice were first crossed to Cre recombinase under the control of the Esr promoter to generate $RhoA^{fl/fl}$-EsrCre mice, which harbor a ubiquitously expressing, tamoxifen (4HT) inducible promoter, to assess specificity for the deletion of RhoA. We generated multiple cell clones from mouse embryonic fibroblasts (MEFs) isolated from either $RhoA^{fl/fl}$ alone or the $RhoA^{fl/fl}$-EsrCre mice. Cells were either left untreated or were treated with tamoxifen to determine effective deletion of RhoA (Supplemental Figure 1B); tamoxifen-treated $RhoA^{fl/fl}$-EsrCre cells had less RhoA than untreated or treated $RhoA^{fl/fl}$ clones. The abundance of other GTPases and Rho family members was normal, indicating that there was specific deletion of RhoA and no compensation by other Rho family members (Supplemental Figure 1B). To assess the role of

RhoA in myocardium specifically, we next crossed the $RhoA^{fl/fl}$ mice to mice expressing Cre recombinase under the control of the α-myosin heavy chain (αMHC) promoter (Supplemental Figure 1C). As expected, hearts isolated from $RhoA^{fl/fl}$-αMHC-Cre (hereafter ($RhoA^{fl/fl}$-Cre) mice showed greater than 90% deletion of RhoA. The protein abundance of RhoA was normal in non-cardiac tissues, such as skeletal muscle, and there was no effect of deletion of RhoA in the total abundance of downstream effectors, such as AKT (Supplemental Figure 1C), suggesting specific cardiomyocyte-deletion of RhoA in these mice. The residual RhoA protein in hearts likely reflects RhoA in other resident cardiac cell types (for example, fibroblasts, vascular endothelial cells, and inflammatory cells).

$RhoA^{fl/fl}$-Cre mice were born at the expected Mendelian ratio and did not have an overt phenotype. Cardiac structure and size were similar in 8-week old $RhoA^{fl/fl}$-Cre and $RhoA^{+/+}$-αMHC-Cre (control) mice (Supplemental Figure 2A). Histological analyses revealed no overt pathology, hypertrophy, or fibrosis in hearts from both lines, as assessed by hematoxylin and eosin (H&E) and Masson's trichrome staining (Supplemental Figure 2B). To determine whether loss of RhoA in cardiomyocytes affects cardiac function, we measured left ventricular posterior wall dimension (LVPWd), chamber dimension (LVDd) and fractional shortening (FS%) by echocardiography and found no significant differences between $RhoA^{fl/fl}$-Cre and control mice (Supplemental Figure 2C). Thus, cardiomyocyte-specific deletion of RhoA in adult mice is not sufficient to induce hypertrophy nor is it inherently pathological in the absence of stress.

Cardiomyocyte-specific deletion of RhoA leads to an accelerated dilated cardiomyopathy following chronic pressure overload

Cardiac overexpression (~20 fold higher) of RhoA leads to dilation and heart failure (13). However, *in vivo* overexpression to a lesser extent (~2 fold higher) of a constitutively active mutant of RhoA is cardioprotective, at least in response to acute ischemia/reperfusion injury (22). To assess the role of RhoA under chronic stress conditions, we subjected control and $RhoA^{fl/fl}$-Cre mice to either 2 or 8-weeks of TAC (Figure 1). Although both control and $RhoA^{fl/fl}$-Cre mice developed the expected compensatory cardiac hypertrophic responses 2-weeks after TAC, we found that $RhoA^{fl/fl}$-Cre mice subjected to 8-weeks of TAC had hearts that were grossly enlarged, with a dilated ventricular chamber, increased heart to body weight ratios, and a tendency to increased lung to body weight ratios, as compared to control mice (Figure 1A, 1B). These mice also had severe cellular pathology, including increased myofiber disarray, enlarged nuclei and increased interstitial space (Supplemental Figure 3). Together, these data suggest that RhoA in cardiomyocytes may be required to sustain compensatory hypertrophy by preventing the transition to dilation in response to chronic stress.

Cardiac-specific deletion of RhoA mice increases the severity of heart failure in response to chronic pressure overload

To confirm the phenotype observed by histology, we performed echocardiography to assess the cardiac function of both control and $RhoA^{fl/fl}$-Cre mice in response to TAC (Figure 1C). After 8 weeks of TAC, left ventricular chamber diameter (LVDd) was significantly

increased and left ventricular posterior wall thickness (LVPWd) was decreased, suggestive of a dilated cardiomyopathy (Figure 1D). Concomitant with these anatomic abnormalities, left ventricular function, as assessed by fractional shortening, was more impaired in $RhoA^{fl/fl}$-Cre mice than in control mice (Figure 1D), suggesting an accelerated transition to heart failure. To validate these findings, we measured the haemodynamic parameters of these mice (Figure 1E). While hearts from control mice showed increased left ventricular pressure (LVP) in response to both 2- and 8- weeks of TAC, indicative of compensatory hypertrophy, the hearts from $RhoA^{fl/fl}$-Cre mice developed increases in both left ventricular pressure and left ventricular volume, suggesting loss of contractility of the heart in these mice and greater cardiac dilation (Figure 1E). In addition, ventricular contractility (dP/dT) minimum and maximum were lower in cardiomyocyte-specific deleted RhoA hearts than in control hearts (Figure 1F), suggesting $RhoA^{fl/fl}$-Cre mice were indeed transitioning to heart failure.

Reactivation of the fetal gene program is a hallmark feature of hypertrophied and failing hearts and correlates with impaired cardiac function and poor prognosis (26). To assess the effects of chronic stress on cardiac disease state, we measured the fetal gene expression profiles in control and cardiomyocyte-specific deleted RhoA mouse hearts at baseline and in response to 2- or 8-weeks of TAC. Both control and $RhoA^{fl/fl}$-Cre hearts showed increased abundance of transcripts encoding atrial natriuretic factor (ANF) and brain natriuretic peptide (BNP). Moreover, in response to TAC, we observed a shift in mRNA expression from the adult αMHC to the fetal βMHC isoform in both controls and $RhoA^{fl/fl}$-Cre hearts, indicating the onset of pathological hypertrophy. The decrease in αMHC expression after 8 weeks of TAC was greater in $RhoA^{fl/fl}$-Cre hearts than in control hearts (Figure 1G). Taken together, these data suggest that loss of RhoA in cardiomyocytes can be deleterious to the heart. Indeed, our data suggest that RhoA in cardiomyocytes is required to prolong the transition from hypertrophy to dilation and heart failure in response to chronic stress.

Cardiac-specific deletion of RhoA is associated with decreased contractility through modulation of calcium handling and myosin light chain activation

In response to pressure overload, we showed that loss of RhoA in cardiomyocytes leads to decreased contractility and accelerated dilated cardiomyopathy. Therefore, we next set out to analyze the downstream signaling pathways affected by RhoA loss in myocardium. In B cells, RhoA is important for BCR-dependent phosphatidylinositol (4,5) bisphosphate (PIP_2) synthesis, phospholipase C (PLC) activation, calcium mobilization, and cell proliferation (27). Moreover, RhoA-activated ROCK promotes the intracellular localization and activation of the protein and lipid phosphatase PTEN, allowing it to convert phosphatidylinositol (3,4,5) triphosphate (PIP_3) to PIP_2 in leukocytes and human embryonic kidney cells (17). PIP_2 is cleaved by PLC to generate inositol triphosphate (IP_3) and diacylglycerol (DAG), two second messengers that mediate intracellular calcium release and hypertrophy and proliferation, respectively(28). To determine whether RhoA regulates similar signaling pathways in cardiomyocytes, we measured the abundance and phosphorylation of these enzymes. In response to TAC and when normalized against GAPDH, the total abundance and phosphorylation of PTEN were significantly increased in hearts from control mice (Fig. 2A). In contrast, PTEN abundance and phosphorylation were

basally higher, but decreased in response to TAC in hearts from RhoA$^{fl/fl}$-Cre mice (Figure 2A). PTEN phosphorylation was similar between mice subjected to sham operation or TAC, regardless of genotype (Fig. 2A). Phosphorylation-dependent activation of PLCβ (29) was also basally higher and decreased in response to TAC in hearts from RhoA$^{fl/fl}$-Cre mice, as compared to hearts from control mice (Figure 2A). Together, these data suggest that RhoA signaling regulates PTEN and PLCβ activity in myocardium.

To directly assess whether loss of RhoA is associated with altered calcium release in cardiomyocytes, we measured the abundance of mRNA encoding the sarco(endo)plasmic reticulum calcium pump (SERCA) in response to TAC (Figure 2B). We found that SERCA mRNA abundance was decreased to a greater extent in hearts from RhoA$^{fl/fl}$-Cre mice than in those from control mice (Figure 2C), suggesting a greater decrease in cardiac function and contractility (30). Next, we measured effects on calcium transient in individual cardiomyocytes left unstimulated or stimulated with endothelin-1 (ET-1), a neurohumoral agonist that mimics chronic stress in the heart (31). Basal and stimulated calcium transients were significantly lower in RhoA$^{fl/fl}$-Cre cardiomyocytes than in control cells (Figure 2C), suggesting that RhoA might be involved in mediating increased calcium cycling in response to cardiac stress. Aberrant calcium handling in the heart leads to contractile dysfunction, arrhythmias, and heart failure (32). To determine whether suppressed calcium transients affect cardiac function and contractility, we measured phosphorylation of myosin light chain (MLC), an enzyme whose activity is necessary for muscle contraction (33) and that is a target of ROCK in smooth muscle cells (34, 35). When normalized to GAPDH, MLC phosphorylation was significantly diminished both basally and in response to TAC in RhoA$^{fl/fl}$-Cre hearts, raising the possibility that decreased contractility in cardiomyocyte-deleted RhoA mice is mediated by decreased MLC activity (Figure 2D).

Loss of RhoA in cardiomyocytes is associated with increased dilation and aberrant ERK and AKT activities

In addition to effects on contractility through IP_3, cleavage of PIP_2 into DAG may directly affect the compensatory hypertrophic signaling response. Activation of DAG leads to phosphorylation and activation of protein kinase C (PKC), which induces hypertrophy through indirect actions on the downstream effectors ERK1/2 and AKT (36, 37). To determine whether loss of RhoA affects PKC activity, we measured phosphorylation-induced activation of PKC (38). The phosphorylation of PKC was basally lower and decreased in RhoA$^{fl/fl}$-Cre hearts in response to TAC than in control hearts (Figure 2E). Further, phosphorylation of ERK1/2 and AKT, indicating activation of these kinases (39, 40) were also lower in response to TAC in RhoA$^{fl/fl}$-Cre hearts as compared to control, suggesting that both pro-hypertrophic (41) and pro-survival signals (42), respectively, are decreased in RhoA$^{fl/fl}$-Cre hearts in response to TAC (Figure 2E). Note that basal activation of AKT was lower in RhoA$^{fl/fl}$-Cre hearts. RhoA also mediates the activation of FAK (6, 43, 44), and its activation in cardiomyocytes induces the activation of AKT in response to stress (15). To determine whether RhoA may be involved in FAK-mediated activation of AKT, we measured FAK phosphorylation in control or RhoA$^{fl/fl}$-Cre hearts in response to TAC. In the absence of RhoA, the phosphorylation of FAK in response to TAC decreased significantly (Figure 2E), suggesting that this may be a possible mechanism for the decreased AKT

activity in these mice. Collectively, these data suggest that loss of RhoA in the myocardium may function to decrease signaling pathways that control cardiac function, thereby causing greater dilation, decreased contractility, and loss of hypertrophic response signals.

RhoA in cardiomyocytes is required for the fibrotic response to pressure overload in the heart

Pathophysiological cardiac hypertrophy and remodeling is usually accompanied by reactive fibrosis. However, although $RhoA^{fl/fl}$-Cre mice showed severe dilated cardiomyopathy, the hearts from these mice had less fibrosis than those from control mice, even after 8 weeks of TAC (Figure 3A, 3B). Moreover, mRNA expression profiles for cardiac pro-fibrotic genes were also decreased in response to TAC in $RhoA^{fl/fl}$-Cre hearts, as compared to controls (Supplemental Figure 4), further suggesting that RhoA signaling potentiates fibrosis in response to cardiac stress. These data also suggest that the signals needed to induce fibrosis are initiated specifically by RhoA signaling in cardiomyocytes. Because $RhoA^{fl/fl}$-Cre hearts were dilated but showed reduced cardiac fibrosis following 8 weeks of TAC, we next assessed whether the effects observed were because of reduced myocyte apoptosis. Indeed, cardiomyocyte apoptosis was significantly reduced in $RhoA^{fl/fl}$-Cre hearts as compared to controls, suggesting that loss of RhoA prevents induction of cardiac cell death in response to TAC (Figure 3C).

To delineate the biochemical mechanism associated with the decreased fibrosis in $RhoA^{fl/fl}$-Cre hearts, we measured the phosphorylation of two downstream effectors of ROCK, LIM domain kinase (LIMK) and the mitogen-activated protein kinase (MAPK) p38. RhoA/ROCK activate LIMK, inducing the conversion of G-actin to F-actin (45). Under baseline conditions, G-actin is associated with myocardial response transcription factors (MRTFs), preventing them from entering the nucleus (46, 47). Mechanical or neurohumoral stimulation induces the polymerization of G-actin into F-actin, reducing the association of MRTFs with G-actin and promoting their nuclear translocation (48), thereby enabling the association of MRTF with SRF to induce transcriptional activation of genes that modulate contractility and induce fibrosis (49) (50). RhoA/ROCK also mediate activation of p38 (51), which leads to the phosphorylation and activation of SRF (52). Basal and TAC-induced activity of LIMK was significantly higher in control hearts than in $RhoA^{fl/fl}$-Cre hearts. Moreover, though control hearts showed significantly increased p38 activity in response to TAC, p38 activity remained at baseline in the $RhoA^{fl/fl}$-Cre hearts (Figure 3D). Finally, we observed an apparent (but not statistically significant) increase in F/G actin ratios following 8 weeks of TAC in hearts from control mice, but not in $RhoA^{fl/fl}$-Cre hearts (Figure 3E), suggesting that the loss of RhoA may prevent the conversion of G actin to F actin in response to TAC. In line with these data, $RhoA^{fl/fl}$-Cre hearts also showed significantly reduced MRTF gene expression and a non-statistically significant decrease in SRF gene expression (Figure 3F).

Taken together, our data reveal that RhoA in cardiomyocytes prolongs compensatory hypertrophy, prevents transition to heart failure, and propagates the activation of fibrosis in response to chronic stress in the heart.

Discussion

Our data demonstrate the necessity for RhoA signaling in the heart and suggest molecular mechanisms that mediate its function specifically in cardiomyocytes to control hypertrophy, contractility and fibrosis (Figure 4). We showed that cardiomyocyte-specific expression of RhoA was not required for normal homeostasis or for the initial compensatory hypertrophic response to stress. However, in response to chronic TAC, loss of cardiomyocyte-specific expression of RhoA caused accelerated dilation of the heart, suggesting RhoA is cardio-protective and required for compensatory hypertrophy regulation and heart failure prevention.

In contrast, other groups have reported that loss of RhoA signaling is actually cardio-protective, with beneficial effects observed following 3-weeks of TAC-induced hypertrophy in mice treated with inhibitors or with global deletions of ROCK1 or ROCK2 (12, 53) or with a cardiomyocyte-specific deletion of ROCK2 (54). There are several possible explanations for these discrepancies. First, while we observed no significant improvement in hypertrophy in our cardiomyocyte-deleted RhoA mice following 2 weeks of TAC, improvements in cardiac hypertrophic parameters as visualized by echocardiography may be apparent after 3 weeks. However, and secondly, because other groups assessed hypertrophy following 3 weeks of TAC, the “protective” effects may actually be the beginning of a transition to dilation. We showed that when pressure overload was extended to 8 weeks (to simulate chronic stress), loss of RhoA potentiated heart failure and accelerated dilation. Third, except for the mice with the cardiomyocyte-specific deletion of ROCK2 (54), which again only showed effects of TAC after 3 weeks, previous studies were conducted *in vitro*, in whole animal deletions of ROCK1/2, or by using ROCK inhibitors that may harbor off-target effects and/or affect multiple cell types. Therefore, our model, in which RhoA was deleted specifically in cardiomyocytes, and in which an extended time course for pressure overload was examined, allowed for investigation of the specific role(s) of RhoA signaling in myocardium.

Calcium signaling is fundamental to cardiac contractility and hypertrophy. We showed that RhoA was involved in mediating increased calcium release in response to cardiac stress. The signaling mechanism(s) underlying RhoA-mediated calcium regulation in cardiomyocytes is complex and likely involves several pathways. For example, IP3 receptor abundance increases in response to pressure overload or neurohumoral stimulation, resulting in hypertrophic calcium signaling and concomitant pathological remodeling (55). In this regard, our data indicated that, in response to TAC, cardiomyocyte-specific expression of RhoA was required to stimulate IP3 and DAG signaling by maintaining basal PTEN abundance and increasing PLC activation, therefore suggesting RhoA may be required to mediate increased calcium signaling in the heart. In support of this hypothesis, muscle-specific inactivation of *Pten* in mice confer beneficial effects in the heart in response to both pressure overload (56) and ischemia/reperfusion injury (57), further suggesting PTEN as a possible downstream effector of RhoA in calcium signaling.

RhoA may also play a key regulatory role in compensatory hypertrophy through ERK and AKT (36, 37). Our data indicated that RhoA in cardiomyocytes promoted the activation of

ERK in response to TAC, which could sustain and prolong the compensatory hypertrophic response to stress and prevent the transition to dilation and failure. In line with this, inhibition of RhoA/ROCK by Y-27632 suppresses phenylephrine-induced phosphorylation of ERK, which results in a decrease in the DNA binding activity of GATA-4, a zinc finger transcription factor necessary to induce cardiac hypertrophy (58). In vascular smooth muscle cells, RhoA-mediated actin cytoskeletal rearrangement is necessary for the translocation of ERK to the nucleus and induction of genes necessary for hypertrophy (59). In addition, platelet-derived growth factor (PDGF)-stimulated as well as stretch-induced ERK activation is diminished in smooth muscle cells in response to ROCK inhibition (60, 61).

Cardiac hypertrophy is accompanied by increased AKT activation (62), and RhoA can mediate the activation of AKT in cardiomyocytes through a pathway involving FAK and PI3K (15). However, RhoA has also been suggested to inhibit AKT signaling; for example, RhoA increases activity of PTEN in neutrophils and fibroblasts, but suppresses PI3K/AKT activities (17, 63). Similarly, AKT activation in endothelial cells and aortic tissue is increased when RhoA and/or ROCK are inhibited (24, 64). In contrast with these previous studies, but in line with our data, Del Re *et al*. suggest that RhoA mediates activation of AKT through FAK in cardiomyocytes in response to stress (15). In this regard, RhoA mediate the activation of FAK (6, 43, 44). Moreover, FAK associates with the regulatory p85 subunit of PI3K, activating it to mediate downstream activation of AKT, thereby implicating FAK in the activation of AKT (15) and in the development of cardiac hypertrophy and survival (65, 66).

We also showed a potential role for RhoA signaling in cardiomyocytes in the development of fibrosis. Hearts from $RhoA^{fl/fl}$-Cre mice showed reduced reactive fibrosis following chronic pressure overload and reduced pathological induction of pro-fibrotic genes. Previous studies have shown that ROCK1 contributes to the development of cardiac fibrosis and induction of fibrogenic cytokines in response to pathological stimuli (12) and that haploinsufficiency of ROCK1 in mice reduces cardiac fibrosis without affecting Ang II–induced hypertension and cardiac hypertrophy (67). However, these findings and our results directly contrast with previous studies showing that inhibition of ROCK1 and ROCK2 with Y27632 and fasudil prevent both myocyte hypertrophy and fibrosis in response to pathological stress in rats and mice (11, 20). Several explanations could account for these differences. First, ROCK inhibitors may not be entirely selective and could exert protecting effects by inhibiting other protein kinases, such as PKC and PKA, at higher concentrations. Secondly, our model only targets RhoA in cardiomyocytes; it is therefore possible that RhoA activity in other cardiac linend ages may be involved in initiating the hypertrophic signaling events that occur in response to stress. Finally, RhoA in cardiomyocytes may be critical for the maintenance, not initiation, of hypertrophy.

We showed that $RhoA^{fl/fl}$-Cre mice had decreased transcriptional activation of genes involved in fibrosis, including MRTF and SRF, suggesting a RhoA-dependent myocardial signaling mechanism necessary to initiate the fibrotic response to stress in the heart. SRF is a ubiquitously distributed transcription factor critical for the control of morphogenetic movements and cell migration during embryonic development and for the regulation of cellular behavior in the adult (50). Induction of cardiomyocyte-specific deletion of SRF

leads to reduced expression of contractile genes and to death within 10 weeks as a result of cardiac dilation and heart failure (68). SRF is regulated by myocardin and MRTFs (MRTFa and MRTFb), cofactors that are necessary for the activation of genes encoding cardiac muscle and smooth muscle contractile proteins (69, 70). Indeed, scar formation and interstitial fibrosis in response to myocardial infarction or angiotensin II infusion, respectively, is decreased in MRTFa null mice (49). However, the fibrotic response to injury promotes infarct healing, as MRTFa null mice develop cardiac rupture (49). We suspect that MRTFs, like RhoA, may affect only the later, more chronic stages of cardiac remodeling.

RhoA regulates many aspects of MRTF and SRF activity and this study links reduced fibrosis to RhoA in cardiomyocytes through modulation of the MRTF–SRF signaling axis. Specifically, RhoA-mediated stimulation of ROCK leads to the activation of profilin and mDiaphanous and the incorporation of G-actin into growing F-actin (50). Simultaneously, activation of RhoA and ROCK leads to phosphorylation of LIMK, which inhibits cofilin-mediated depolymerization of F-actin (71), further potentiating the nuclear accumulation of MRTFs and activation of SRF target genes. Lastly, MRTF activity is linked to TGF-β1, a proinflammatory cytokine that mediates the development of fibrosis, and mice expressing constitutively active ROCK develop fibrotic cardiomyopathy with diastolic dysfunction due to activated TGFβ1 and NF-κB (72).

In addition, our findings that cardiomycoyte-specific deletion of RhoA reduced cardiac fibrosis resembles other studies in which mice with cardiac-specific overexpression of dominant negative forms of p38α and p38β develop cardiac hypertrophy but not cardiomyocyte fibrosis in response to pressure overload (73). In addition, transgenic mice with cardiac-specific overexpression of the direct upstream activators of p38, MKK3bE or MKK6bE, develop cardiac fibrosis and systolic and diastolic dysfunction but not cardiac hypertrophy (74), further implicating p38 signaling in the development of fibrosis but not hypertrophy. Moreover, p38 inhibition improves cardiac function and attenuates cardiac remodeling following MI (75). Our data indicated that loss of RhoA in cardiomyocytes reduced p38 activity in response to TAC, suggesting an additional mechanism of regulating fibrosis. Indeed, p38 is a target of RhoA in non-cardiac cells (76) and in diabetic and failing mouse hearts (77, 78).

In conclusion, our data reveal that RhoA in cardiomyocytes can have both cardio-protective and cardio-deleterious: it prolongs compensatory hypertrophy and prevent transition to dilation and failure, but can also initiate the fibrotic response in a stressed heart.

Materials and Methods

Generation of $RhoA^{F/F}$;αMHC-Cre mice

RhoA loxP-targeted ($RhoA^{fl/fl}$) mice were generated by Dr. Chris Carpenter, in which exon 3 was flanked by loxP sites to allow tissue-specific deletion (Supplemental Figure 1). These mice were then bred to C57/Bl6J mice expressing Cre recombinase under the control of the tamoxifen inducible estrogen receptor 1a (Esr) promoter (Jackson labs) or Cre recombinase under the control of the α-myosin heavy chain (αMHC) promoter (Dr. Dale Abel, University of Iowa) to generate cardiomyocyte-specific deletion of RhoA ($RhoA^{fl/fl}$-αMHC-

Cre). For all experiments herein, αMHC-Cre alone ($RhoA^{+/+}$-αMHC-Cre) mice were used as controls.

Animal Procedures

All procedures were performed in accordance with the NIH Guide for the Care and Use of Laboratory Animals and approved by the Institutional Animal Care and Use Committee at BIDMC.

Histology

Hearts for morphometry and histochemistry were flushed with PBS, perfusion fixed in Bouin's reagent, and paraffin embedded. Sections (5 μm) were stained with H&E, Masson-Trichrome, or reticulin at the Rodent Histopathology Core (Dr. Roderick Bronson, Harvard Medical School). Cross sectional area of cardiomyocytes with centrally located nuclei (to ensure the same plane of sectioning) were measured using ImageJ 1.41 software (developed by Wayne Rasband; http://rsbweb.nih.gov/ij/). 200–500 cells were measured for each genotype. Masson's trichrome stain, which stains collagen fibers blue, was used to quantify fibrosis. Images of the whole heart section were obtained and quantified on a Keyence BZ-9000 Microscope. Percentages of fibrotic area were obtained by dividing fibrosis area by the total ventricular area.

Quantitative real-time PCR

RNA was isolated from whole hearts with using the RNeasy Mini Kit (QIAGEN). Quantitative real-time PCR was performed with SYBR Green (Applied Biosystems), using an Applied Biosystems 7900. Gene expression analyses were carried out according to the manufacturer's instructions. Primer sequences and conditions are listed in Supplemental Table 1. Each measurement was obtained using at least 3 mice per group, and each sample was measured in triplicate. Data were quantified by using the comparative CT method, with *Gapdh* and *RPL13* expression as a control.

Echocardiography

Transthoracic echocardiography was conducted on non-anesthetized animals as described previously (79), with a 13-MHz probe (Vivid 7, GE Medical Systems, Boston, MA) or VisualSonics Vevo 770 high-frequency ultrasound rodent imaging system (VisualSonics). GE Medical Systems or VisualSonics Vevo 770 software was used for data acquisition and subsequent analysis. Hearts were imaged in the 2-dimensional parasternal short-axis view, and an M-mode echocardiogram of the midventricular region was recorded at the level of the papillary muscles. Calculations of cardiac anatomic and functional parameters were carried out as described previously (79).

Transverse aortic constriction and Hemodynamic studies

Transverse aortic banding was performed on anesthetized 16 week-old male mice (n=4–6 mice per group at each time point). The ligature for aortic banding was sized by tying around a 25-gauge needle. The ligature was placed on the transverse aorta between the brachiocephalic trunk and the left common carotid artery. Sham-operated control mice

underwent the entire operative procedure without aortic banding. Cardiac function was evaluated by measuring the maximum rate of increase (dP/dtmax) and decline (dP/dtmin) in left ventricular pressure with a micromanometer catheter (Millar 1.4F, SPR 671, Millar Instruments) positioned in the left ventricle via a right common carotid artery cannulation.

Ca^{2+} Measurements in Adult Cardiomyocytes

Adult cardiomyocytes were isolated from αMHC-Cre or $RhoA^{F/F}$-αMHC-Cre mice as previously described (80). Briefly, whole hearts were perfused with a Tyrode's solution containing liberase blendzyme (Roche) at 37°C. Following cardiac perfusion, the ventricles were disassociated into individual myocytes, filtered and Ca^{2+} reintroduced and plated in laminin coated glass bottom dishes (MatTek). Myocytes were loaded with 2 μM Fura-2 AM (Invitrogen) and pluronic acid for 15 minutes in M199 media with 2,3-butanedione monoxime (Sigma) at room temperature. Cells were then washed and bathed in Ringer's solution and electrically stimulated Ca^{2+} transients were acquired using a DeltaRam spectrofluorophotometer (Photon Technology International), operated at an emission wavelength of 510 nm, with excitation wavelengths of 340 and 380 nm. The myocytes were continuously paced at 0.5Hz for 60s in the presence of Ringer's solution followed by 4 minutes in the presence of Ringers solution with 100nM endothelin (Total perfusion time 300s). Ca^{2+}transients from 50–60s were averaged to obtain naive Ca^{2+} transient amplitude and Ca^{2+} transients from 290–300s were averaged to obtain endothelin stimulated Ca^{2+} transient amplitude. Percent change in the amplitude of Ca^{2+} transient was calculated by taking the difference between naïve and endothelin stimulated Ca^{2+} transient amplitude over naïve Ca^{2+} transient amplitude. Data were analyzed using Felix (Photon Technology International) and Clampfit (Molecular Devices) software.

Biochemical analyses

Whole hearts from αMHC-Cre or $RhoA^{F/F}$-αMHC-Cre mice were dissected, perfused in PBS, and immediately frozen in liquid N2. Whole-cell lysates were prepared by homogenizing the tissue in radioimmunoprecipitation (RIPA) buffer (25 mmol/l Tris-HCl [pH 7.4], 150 mmol/l NaCl, 0.1% SDS, 1% NP-40, 0.5% sodium deoxycholate, 5 mmol/l EDTA, 1 mmol/l NaF, 1 mmol/l sodium orthovanadate, and a protease cocktail) at 4°C, followed by clarification at 14,000 g. Proteins were resolved by SDS-PAGE and transferred to PVDF membranes. Immunoblots were performed, following the manufacturer's directions, with anti-Akt (sc-8312), anti-phospho-FAK (sc-16563), anti-FAK (sc-558), anti-LIMK (sc-5576), or pLIMK (sc-28409) antibodies (from Santa Cruz Biotechnology Inc.); or anti-phospho-Akt (9271), anti-phospho-Erk1/2 (9101), anti-Erk1/2 (9102), anti-phospho-PTEN (9554), anti-phospho-PLCb, anti-phospho-MLC (3671), anti-PTEN (9188), anti-phospho-PKC (9379), anti-PKC (2056), anti-phospho-p38 (4511), or anti-p38 (9212) antibodies (all from Cell Signaling Technology); or anti-PLCb (ABS512) antibodies (from Millipore). Bands were visualized with enhanced chemiluminescence and quantified by densitometry (ImageJ 1.41 software).

F/G actin ratio measurements

F-actin/G-actin ratios from control and $RhoA^{fl/fl}$-Cre mouse hearts were assessed using animals that received sham operation or TAC for 8 weeks. Analysis of the F-Actin/G-actin

was generated using the In Vivo Assay Biochem Kit (Cytoskeleton Inc)and experiments were conducted according to the manufacturer instructions. Briefly, cells were lysed in a detergent based lysis buffer that stabilized and maintained the F and G forms of cellular actin. G actin was solubilized, whereas the insoluble F actin was pelleted by centrifugation. Samples of supernatant and pellet were visualized by SDS PAGE and the relative ratio of F to G actin was quantitated by western blot analysis using ImageJ. Samples from n=3 mice/ group were run in triplicates.

Statistics

All data are expressed as mean ± SEM. Statistical significance was determined using 2-tailed Student's t test and 1-way ANOVA or 2-way repeated measure ANOVA, as appropriate. If ANOVA was significant, individual differences were evaluated using the Bonferroni post-test. For all studies, values of $p<0.05$ were considered statistically significant. Statistical analysis was validated by Drs. Murray Mittleman and Erin Reese, through the support of Harvard Catalyst and The Harvard Clinical and Translational Science Center.

Supplementary Material

Refer to Web version on PubMed Central for supplementary material.

Acknowledgments

We would like to thank Dr. Lewis Cantley for helpful discussions and for providing us with the $RhoA^{fl/fl}$ mice. In addition, we would like to thank Drs. Eleni and Charalampia Geladari from the Kontaridis lab for their helpful discussions. We would also like to thank Dr. Dale Abel, at the University of Iowa, for providing us with the αMHC-Cre mouse model. Finally, we would also like to thank and acknowledge Drs. Murray Mittleman and Erin Reese, who validated the statistical methodology herein.

Funding: This work was supported by National Institutes of Health Grants R01-HL102368 and R01-HL114775 to M.I.K and by an American Heart Association Postdoctoral fellowship to J.L. This work was also supported in part by the Beth Israel Deaconess Medical Center Division of Cardiology. Statistical analysis conducted in the manuscript was validated through support by Harvard Catalyst, The Harvard Clinical and Translational Science Center (National Center for Research Resources and the National Center for Advancing Translational Sciences, National Institutes of Health Award UL1 TR001102) and financial contributions from Harvard University and its affiliated academic healthcare centers. The content is solely the responsibility of the authors and does not necessarily represent the official views of Harvard Catalyst, Harvard University and its affiliated academic healthcare centers, or the National Institutes of Health.

References and Notes

1. Yung CK, Halperin VL, Tomaselli GF, Winslow RL. Gene expression profiles in end-stage human idiopathic dilated cardiomyopathy: altered expression of apoptotic and cytoskeletal genes. Genomics. 2004; 83:281–297. [PubMed: 14706457]
2. Richardson P, McKenna W, Bristow M, Maisch B, Mautner B, O'Connell J, Olsen E, Thiene G, Goodwin J, Gyarfas I, Martin I, Nordet P. Report of the 1995 World Health Organization/ International Society and Federation of Cardiology Task Force on the Definition and Classification of cardiomyopathies. Circulation. 1996; 93:841–842. [PubMed: 8598070]
3. Chien KR. Stress pathways and heart failure. Cell. 1999; 98:555–558. [PubMed: 10490095]
4. Mackay DJ, Hall A. Rho GTPases. J Biol Chem. 1998; 273:20685–20688. [PubMed: 9694808]
5. Brown JH, Del Re DP, Sussman MA. The Rac and Rho hall of fame: a decade of hypertrophic signaling hits. Circ Res. 2006; 98:730–742. [PubMed: 16574914]

6. Hoshijima M, Sah VP, Wang Y, Chien KR, Brown JH. The low molecular weight GTPase Rho regulates myofibril formation and organization in neonatal rat ventricular myocytes. Involvement of Rho kinase. J Biol Chem. 1998; 273:7725–7730. [PubMed: 9516480]
7. Kimura K, Ito M, Amano M, Chihara K, Fukata Y, Nakafuku M, Yamamori B, Feng J, Nakano T, Okawa K, Iwamatsu A, Kaibuchi K. Regulation of myosin phosphatase by Rho and Rho-associated kinase (Rho-kinase). Science. 1996; 273:245–248. [PubMed: 8662509]
8. Noma K, Oyama N, Liao JK. Physiological role of ROCKs in the cardiovascular system. Am J Physiol Cell Physiol. 2006; 290:C661–668. [PubMed: 16469861]
9. Lin G, Craig GP, Zhang L, Yuen VG, Allard M, McNeill JH, MacLeod KM. Acute inhibition of Rho-kinase improves cardiac contractile function in streptozotocin-diabetic rats. Cardiovasc Res. 2007; 75:51–58. [PubMed: 17428455]
10. Phrommintikul A, Tran L, Kompa A, Wang B, Adrahtas A, Cantwell D, Kelly DJ, Krum H. Effects of a Rho kinase inhibitor on pressure overload induced cardiac hypertrophy and associated diastolic dysfunction. Am J Physiol Heart Circ Physiol. 2008; 294:H1804–1814. [PubMed: 18245565]
11. Higashi M, Shimokawa H, Hattori T, Hiroki J, Mukai Y, Morikawa K, Ichiki T, Takahashi S, Takeshita A. Long-term inhibition of Rho-kinase suppresses angiotensin II-induced cardiovascular hypertrophy in rats in vivo: effect on endothelial NAD(P)H oxidase system. Circ Res. 2003; 93:767–775. [PubMed: 14500337]
12. Zhang YM, Bo J, Taffet GE, Chang J, Shi J, Reddy AK, Michael LH, Schneider MD, Entman ML, Schwartz RJ, Wei L. Targeted deletion of ROCK1 protects the heart against pressure overload by inhibiting reactive fibrosis. FASEB J. 2006; 20:916–925. [PubMed: 16675849]
13. Sah VP, Minamisawa S, Tam SP, Wu TH, Dorn GW 2nd, Ross J Jr, Chien KR, Brown JH. Cardiac-specific overexpression of RhoA results in sinus and atrioventricular nodal dysfunction and contractile failure. J Clin Invest. 1999; 103:1627–1634. [PubMed: 10377168]
14. Shi J, Zhang YW, Summers LJ, Dorn GW 2nd, Wei L. Disruption of ROCK1 gene attenuates cardiac dilation and improves contractile function in pathological cardiac hypertrophy. J Mol Cell Cardiol. 2008; 44:551–560. [PubMed: 18178218]
15. Del Re DP, Miyamoto S, Brown JH. Focal adhesion kinase as a RhoA-activable signaling scaffold mediating Akt activation and cardiomyocyte protection. J Biol Chem. 2008; 283:35622–35629. [PubMed: 18854312]
16. Sugimoto N, Takuwa N, Yoshioka K, Takuwa Y. Rho-dependent, Rho kinase-independent inhibitory regulation of Rac and cell migration by LPA1 receptor in Gi-inactivated CHO cells. Exp Cell Res. 2006; 312:1899–1908. [PubMed: 16564043]
17. Li Z, Dong X, Wang Z, Liu W, Deng N, Ding Y, Tang L, Hla T, Zeng R, Li L, Wu D. Regulation of PTEN by Rho small GTPases. Nat Cell Biol. 2005; 7:399–404. [PubMed: 15793569]
18. Guan SJ, Ma ZH, Wu YL, Zhang JP, Liang F, Weiss JW, Guo QY, Wang JY, Ji ES, Chu L. Long-term administration of fasudil improves cardiomyopathy in streptozotocin-induced diabetic rats. Food and chemical toxicology : an international journal published for the British Industrial Biological Research Association. 2012; 50:1874–1882. [PubMed: 22429817]
19. Satoh S, Ueda Y, Koyanagi M, Kadokami T, Sugano M, Yoshikawa Y, Makino N. Chronic inhibition of Rho kinase blunts the process of left ventricular hypertrophy leading to cardiac contractile dysfunction in hypertension-induced heart failure. J Mol Cell Cardiol. 2003; 35:59–70. [PubMed: 12623300]
20. Hattori T, Shimokawa H, Higashi M, Hiroki J, Mukai Y, Tsutsui H, Kaibuchi K, Takeshita A. Long-term inhibition of Rho-kinase suppresses left ventricular remodeling after myocardial infarction in mice. Circulation. 2004; 109:2234–2239. [PubMed: 15096457]
21. Kobayashi N, Horinaka S, Mita S, Nakano S, Honda T, Yoshida K, Kobayashi T, Matsuoka H. Critical role of Rho-kinase pathway for cardiac performance and remodeling in failing rat hearts. Cardiovasc Res. 2002; 55:757–767. [PubMed: 12176125]
22. Xiang SY, Vanhoutte D, Del Re DP, Purcell NH, Ling H, Banerjee I, Bossuyt J, Lang RA, Zheng Y, Matkovich SJ, Miyamoto S, Molkentin JD, Dorn GW 2nd, Brown JH. RhoA protects the mouse heart against ischemia/reperfusion injury. J Clin Invest. 2011; 121:3269–3276. [PubMed: 21747165]

23. Bao W, Hu E, Tao L, Boyce R, Mirabile R, Thudium DT, Ma XL, Willette RN, Yue TL. Inhibition of Rho-kinase protects the heart against ischemia/reperfusion injury. Cardiovasc Res. 2004; 61:548–558. [PubMed: 14962485]
24. Wolfrum S, Dendorfer A, Rikitake Y, Stalker TJ, Gong Y, Scalia R, Dominiak P, Liao JK. Inhibition of Rho-kinase leads to rapid activation of phosphatidylinositol 3-kinase/protein kinase Akt and cardiovascular protection. Arterioscler Thromb Vasc Biol. 2004; 24:1842–1847. [PubMed: 15319269]
25. Rajashree R, Blunt BC, Hofmann PA. Modulation of myosin phosphatase targeting subunit and protein phosphatase 1 in the heart. Am J Physiol Heart Circ Physiol. 2005; 289:H1736–1743. [PubMed: 15908465]
26. Kuwahara K, Saito Y, Takano M, Arai Y, Yasuno S, Nakagawa Y, Takahashi N, Adachi Y, Takemura G, Horie M, Miyamoto Y, Morisaki T, Kuratomi S, Noma A, Fujiwara H, Yoshimasa Y, Kinoshita H, Kawakami R, Kishimoto I, Nakanishi M, Usami S, Saito Y, Harada M, Nakao K. NRSF regulates the fetal cardiac gene program and maintains normal cardiac structure and function. EMBO J. 2003; 22:6310–6321. [PubMed: 14633990]
27. Saci A, Carpenter CL. RhoA GTPase regulates B cell receptor signaling. Mol Cell. 2005; 17:205–214. [PubMed: 15664190]
28. Gomez AM, Ruiz-Hurtado G, Benitah JP, Dominguez-Rodriguez A. Ca(2+) fluxes involvement in gene expression during cardiac hypertrophy. Curr Vasc Pharmacol. 2013; 11:497–506. [PubMed: 23905644]
29. Vitale M, Matteucci A, Manzoli L, Rodella L, Mariani AR, Zauli G, Falconi M, Billi AM, Martelli AM, Gilmour RS, Cocco L. Interleukin 2 activates nuclear phospholipase Cbeta by mitogen-activated protein kinase-dependent phosphorylation in human natural killer cells. FASEB J. 2001; 15:1789–1791. [PubMed: 11481231]
30. Park WJ, Oh JG. SERCA2a: a prime target for modulation of cardiac contractility during heart failure. BMB reports. 2013; 46:237–243. [PubMed: 23710633]
31. Drawnel FM, Archer CR, Roderick HL. The role of the paracrine/autocrine mediator endothelin-1 in regulation of cardiac contractility and growth. Br J Pharmacol. 2013; 168:296–317. [PubMed: 22946456]
32. Bers DM, Despa S. Cardiac myocytes Ca2+ and Na+ regulation in normal and failing hearts. Journal of pharmacological sciences. 2006; 100:315–322. [PubMed: 16552170]
33. Kamm KE, Stull JT. Signaling to myosin regulatory light chain in sarcomeres. J Biol Chem. 2011; 286:9941–9947. [PubMed: 21257758]
34. Noma K, Rikitake Y, Oyama N, Yan G, Alcaide P, Liu PY, Wang H, Ahl D, Sawada N, Okamoto R, Hiroi Y, Shimizu K, Luscinskas FW, Sun J, Liao JK. ROCK1 mediates leukocyte recruitment and neointima formation following vascular injury. J Clin Invest. 2008; 118:1632–1644. [PubMed: 18414683]
35. Wang Y, Zheng XR, Riddick N, Bryden M, Baur W, Zhang X, Surks HK. ROCK isoform regulation of myosin phosphatase and contractility in vascular smooth muscle cells. Circ Res. 2009; 104:531–540. [PubMed: 19131646]
36. Selvetella G, Hirsch E, Notte A, Tarone G, Lembo G. Adaptive and maladaptive hypertrophic pathways: points of convergence and divergence. Cardiovascular research. 2004; 63:373–380. [PubMed: 15276462]
37. Aikawa R, Komuro I, Yamazaki T, Zou Y, Kudoh S, Zhu W, Kadowaki T, Yazaki Y. Rho family small G proteins play critical roles in mechanical stress-induced hypertrophic responses in cardiac myocytes. Circ Res. 1999; 84:458–466. [PubMed: 10066681]
38. Keranen LM, Dutil EM, Newton AC. Protein kinase C is regulated in vivo by three functionally distinct phosphorylations. Curr Biol. 1995; 5:1394–1403. [PubMed: 8749392]
39. Cobb MH, Goldsmith EJ. How MAP kinases are regulated. J Biol Chem. 1995; 270:14843–14846. [PubMed: 7797459]
40. Bos JL. A target for phosphoinositide 3-kinase: Akt/PKB. Trends Biochem Sci. 1995; 20:441–442. [PubMed: 8578585]
41. Molkentin JD. Calcineurin-NFAT signaling regulates the cardiac hypertrophic response in coordination with the MAPKs. Cardiovasc Res. 2004; 63:467–475. [PubMed: 15276472]

42. Tucka J, Bennett M, Littlewood T. Cell death and survival signalling in the cardiovascular system. Frontiers in bioscience. 2012; 17:248–261.
43. Torsoni AS, Marin TM, Velloso LA, Franchini KG. RhoA/ROCK signaling is critical to FAK activation by cyclic stretch in cardiac myocytes. Am J Physiol Heart Circ Physiol. 2005; 289:H1488–1496. [PubMed: 15923313]
44. Heidkamp MC, Bayer AL, Scully BT, Eble DM, Samarel AM. Activation of focal adhesion kinase by protein kinase C epsilon in neonatal rat ventricular myocytes. Am J Physiol Heart Circ Physiol. 2003; 285:H1684–1696. [PubMed: 12829427]
45. Arber S, Barbayannis FA, Hanser H, Schneider C, Stanyon CA, Bernard O, Caroni P. Regulation of actin dynamics through phosphorylation of cofilin by LIM-kinase. Nature. 1998; 393:805–809. [PubMed: 9655397]
46. Miralles F, Posern G, Zaromytidou AI, Treisman R. Actin dynamics control SRF activity by regulation of its coactivator MAL. Cell. 2003; 113:329–342. [PubMed: 12732141]
47. Guettler S, Vartiainen MK, Miralles F, Larijani B, Treisman R. RPEL motifs link the serum response factor cofactor MAL but not myocardin to Rho signaling via actin binding. Mol Cell Biol. 2008; 28:732–742. [PubMed: 18025109]
48. Hinson JS, Medlin MD, Lockman K, Taylor JM, Mack CP. Smooth muscle cell-specific transcription is regulated by nuclear localization of the myocardin-related transcription factors. Am J Physiol Heart Circ Physiol. 2007; 292:H1170–1180. [PubMed: 16997888]
49. Small EM, Thatcher JE, Sutherland LB, Kinoshita H, Gerard RD, Richardson JA, Dimaio JM, Sadek H, Kuwahara K, Olson EN. Myocardin-related transcription factor-a controls myofibroblast activation and fibrosis in response to myocardial infarction. Circ Res. 2010; 107:294–304. [PubMed: 20558820]
50. Small EM. The actin-MRTF-SRF gene regulatory axis and myofibroblast differentiation. Journal of cardiovascular translational research. 2012; 5:794–804. [PubMed: 22898751]
51. Lopez-Ilasaca M. Signaling from G-protein-coupled receptors to mitogen-activated protein (MAP)-kinase cascades. Biochem Pharmacol. 1998; 56:269–277. [PubMed: 9744561]
52. Heidenreich O, Neininger A, Schratt G, Zinck R, Cahill MA, Engel K, Kotlyarov A, Kraft R, Kostka S, Gaestel M, Nordheim A. MAPKAP kinase 2 phosphorylates serum response factor in vitro and in vivo. J Biol Chem. 1999; 274:14434–14443. [PubMed: 10318869]
53. Hamid SA, Bower HS, Baxter GF. Rho kinase activation plays a major role as a mediator of irreversible injury in reperfused myocardium. Am J Physiol Heart Circ Physiol. 2007; 292:H2598–2606. [PubMed: 17220176]
54. Okamoto R, Li Y, Noma K, Hiroi Y, Liu PY, Taniguchi M, Ito M, Liao JK. FHL2 prevents cardiac hypertrophy in mice with cardiac-specific deletion of ROCK2. FASEB J. 2013; 27:1439–1449. [PubMed: 23271052]
55. Drawnel FM, Wachten D, Molkentin JD, Maillet M, Aronsen JM, Swift F, Sjaastad I, Liu N, Catalucci D, Mikoshiba K, Hisatsune C, Okkenhaug H, Andrews SR, Bootman MD, Roderick HL. Mutual antagonism between IP(3)RII and miRNA-133a regulates calcium signals and cardiac hypertrophy. J Cell Biol. 2012; 199:783–798. [PubMed: 23166348]
56. Oudit GY, Kassiri Z, Zhou J, Liu QC, Liu PP, Backx PH, Dawood F, Crackower MA, Scholey JW, Penninger JM. Loss of PTEN attenuates the development of pathological hypertrophy and heart failure in response to biomechanical stress. Cardiovasc Res. 2008; 78:505–514. [PubMed: 18281373]
57. Ruan H, Li J, Ren S, Gao J, Li G, Kim R, Wu H, Wang Y. Inducible and cardiac specific PTEN inactivation protects ischemia/reperfusion injury. J Mol Cell Cardiol. 2009; 46:193–200. [PubMed: 19038262]
58. Yanazume T, Hasegawa K, Wada H, Morimoto T, Abe M, Kawamura T, Sasayama S. Rho/ROCK pathway contributes to the activation of extracellular signal-regulated kinase/GATA-4 during myocardial cell hypertrophy. J Biol Chem. 2002; 277:8618–8625. [PubMed: 11739382]
59. Kawamura S, Miyamoto S, Brown JH. Initiation and transduction of stretch-induced RhoA and Rac1 activation through caveolae: cytoskeletal regulation of ERK translocation. J Biol Chem. 2003; 278:31111–31117. [PubMed: 12777392]

60. Kamiyama M, Utsunomiya K, Taniguchi K, Yokota T, Kurata H, Tajima N, Kondo K. Contribution of Rho A and Rho kinase to platelet-derived growth factor-BB-induced proliferation of vascular smooth muscle cells. Journal of atherosclerosis and thrombosis. 2003; 10:117–123. [PubMed: 12740486]
61. Zeidan A, Nordstrom I, Albinsson S, Malmqvist U, Sward K, Hellstrand P. Stretch-induced contractile differentiation of vascular smooth muscle: sensitivity to actin polymerization inhibitors. Am J Physiol Cell Physiol. 2003; 284:C1387–1396. [PubMed: 12734104]
62. Del Re DP, Miyamoto S, Brown JH. RhoA/Rho kinase up-regulate Bax to activate a mitochondrial death pathway and induce cardiomyocyte apoptosis. J Biol Chem. 2007; 282:8069–8078. [PubMed: 17234627]
63. Sanchez T, Thangada S, Wu MT, Kontos CD, Wu D, Wu H, Hla T. PTEN as an effector in the signaling of antimigratory G protein-coupled receptor. Proc Natl Acad Sci U S A. 2005; 102:4312–4317. [PubMed: 15764699]
64. Eto M, Kozai T, Cosentino F, Joch H, Luscher TF. Statin prevents tissue factor expression in human endothelial cells: role of Rho/Rho-kinase and Akt pathways. Circulation. 2002; 105:1756–1759. [PubMed: 11956113]
65. Eble DM, Strait JB, Govindarajan G, Lou J, Byron KL, Samarel AM. Endothelin-induced cardiac myocyte hypertrophy: role for focal adhesion kinase. Am J Physiol Heart Circ Physiol. 2000; 278:H1695–1707. [PubMed: 10775151]
66. Clemente CF, Tornatore TF, Theizen TH, Deckmann AC, Pereira TC, Lopes-Cendes I, Souza JR, Franchini KG. Targeting focal adhesion kinase with small interfering RNA prevents and reverses load-induced cardiac hypertrophy in mice. Circ Res. 2007; 101:1339–1348. [PubMed: 17947798]
67. Rikitake Y, Oyama N, Wang CY, Noma K, Satoh M, Kim HH, Liao JK. Decreased perivascular fibrosis but not cardiac hypertrophy in ROCK1+/− haploinsufficient mice. Circulation. 2005; 112:2959–2965. [PubMed: 16260635]
68. Parlakian A, Charvet C, Escoubet B, Mericskay M, Molkentin JD, Gary-Bobo G, De Windt LJ, Ludosky MA, Paulin D, Daegelen D, Tuil D, Li Z. Temporally controlled onset of dilated cardiomyopathy through disruption of the SRF gene in adult heart. Circulation. 2005; 112:2930–2939. [PubMed: 16260633]
69. Wang D, Chang PS, Wang Z, Sutherland L, Richardson JA, Small E, Krieg PA, Olson EN. Activation of cardiac gene expression by myocardin, a transcriptional cofactor for serum response factor. Cell. 2001; 105:851–862. [PubMed: 11439182]
70. Du KL, Ip HS, Li J, Chen M, Dandre F, Yu W, Lu MM, Owens GK, Parmacek MS. Myocardin is a critical serum response factor cofactor in the transcriptional program regulating smooth muscle cell differentiation. Mol Cell Biol. 2003; 23:2425–2437. [PubMed: 12640126]
71. Sotiropoulos A, Gineitis D, Copeland J, Treisman R. Signal-regulated activation of serum response factor is mediated by changes in actin dynamics. Cell. 1999; 98:159–169. [PubMed: 10428028]
72. Yang X, Li Q, Lin X, Ma Y, Yue X, Tao Z, Wang F, McKeehan WL, Wei L, Schwartz RJ, Chang J. Mechanism of fibrotic cardiomyopathy in mice expressing truncated Rho-associated coiled-coil protein kinase 1. FASEB J. 2012; 26:2105–2116. [PubMed: 22278938]
73. Zhang S, Weinheimer C, Courtois M, Kovacs A, Zhang CE, Cheng AM, Wang Y, Muslin AJ. The role of the Grb2-p38 MAPK signaling pathway in cardiac hypertrophy and fibrosis. J Clin Invest. 2003; 111:833–841. [PubMed: 12639989]
74. Liao P, Georgakopoulos D, Kovacs A, Zheng M, Lerner D, Pu H, Saffitz J, Chien K, Xiao RP, Kass DA, Wang Y. The in vivo role of p38 MAP kinases in cardiac remodeling and restrictive cardiomyopathy. Proc Natl Acad Sci U S A. 2001; 98:12283–12288. [PubMed: 11593045]
75. See F, Thomas W, Way K, Tzanidis A, Kompa A, Lewis D, Itescu S, Krum H. p38 mitogen-activated protein kinase inhibition improves cardiac function and attenuates left ventricular remodeling following myocardial infarction in the rat. J Am Coll Cardiol. 2004; 44:1679–1689. [PubMed: 15489104]
76. Kacimi R, Gerdes AM. Alterations in G protein and MAP kinase signaling pathways during cardiac remodeling in hypertension and heart failure. Hypertension. 2003; 41:968–977. [PubMed: 12642504]

77. Ren J, Duan J, Thomas DP, Yang X, Sreejayan N, Sowers JR, Leri A, Kajstura J, Gao F, Anversa P. IGF-I alleviates diabetes-induced RhoA activation, eNOS uncoupling, and myocardial dysfunction. Am J Physiol Regul Integr Comp Physiol. 2008; 294:R793–802. [PubMed: 18199585]

78. Roussel E, Gaudreau M, Plante E, Drolet MC, Breault C, Couet J, Arsenault M. Early responses of the left ventricle to pressure overload in Wistar rats. Life Sci. 2008; 82:265–272. [PubMed: 18155733]

79. Marin TM, Keith K, Davies B, Conner DA, Guha P, Kalaitzidis D, Wu X, Lauriol J, Wang B, Bauer M, Bronson R, Franchini KG, Neel BG, Kontaridis MI. Rapamycin reverses hypertrophic cardiomyopathy in a mouse model of LEOPARD syndrome-associated PTPN11 mutation. J Clin Invest. 2011; 121:1026–1043. [PubMed: 21339643]

80. Goonasekera SA, Molkentin JD. Unraveling the secrets of a double life: contractile versus signaling Ca2+ in a cardiac myocyte. J Mol Cell Cardiol. 2012; 52:317–322. [PubMed: 21600216]

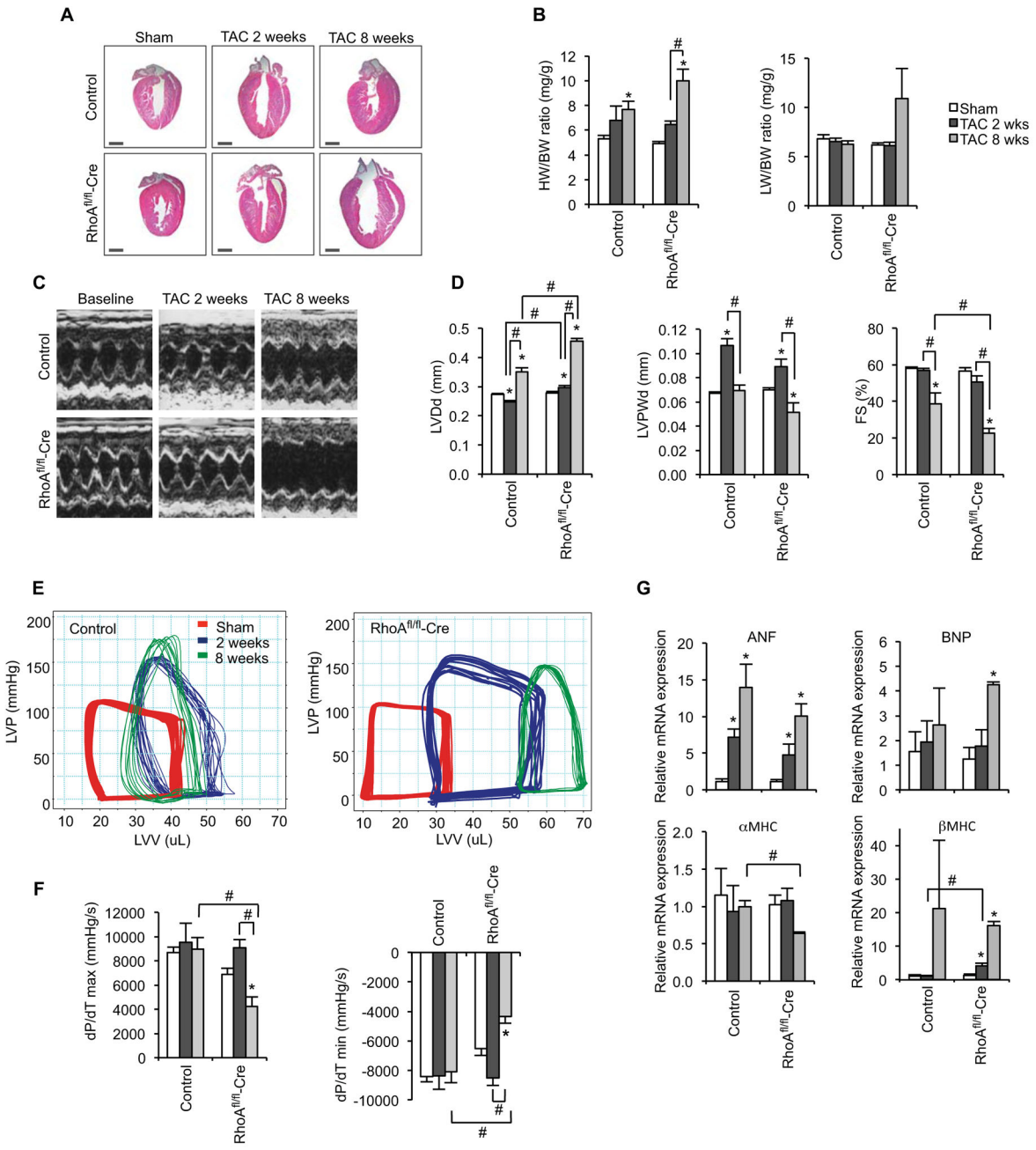

Figure 1. Mice with cardiomyocyte-specific deletion of RhoA develop dilated cardiomyopathy, with decreased heart function and accelerated heart failure in response to chronic pressure overload

Control and RhoA$^{fl/fl}$-Cre mice were subjected to either sham operation or TAC for 2 or 8 weeks. (A) Representative longitudinal heart sections stained with H&E. Scale bar, 0.1mm. (B) Heart to body weight (HW/BW) and lung to body weight (LW/BW) ratios. (C) Representative echocardiographs and corresponding quantification of left ventricular end dimension in diastole (LVEDd), left ventricular posterior wall thickeness in diastole (LVPWd), and fractional shortening (FS). (D) Representative pressure-volume loops and corresponding hemodynamic assessment of contraction velocities (maximum and minimum

pressure difference over time [dP/dt]). (E) qRT-PCR analysis of hypertrophy-related gene expression, which was normalized to *RPL13* mRNA. Results were normalized to sham-operated mice of the same genotype. Samples were obtained from 3 mice per group and each sample was assessed in technical triplicate. n=4–6 mice/group for data in (A), (B), (C), (D), and n=3–4 mice/group for data in (E). Data in graphs represent mean ± SEM; *$p<0.05$, as compared to corresponding shams and #$p<0.05$. All p values were derived from ANOVA and Bonferroni post-test when ANOVA was significant.

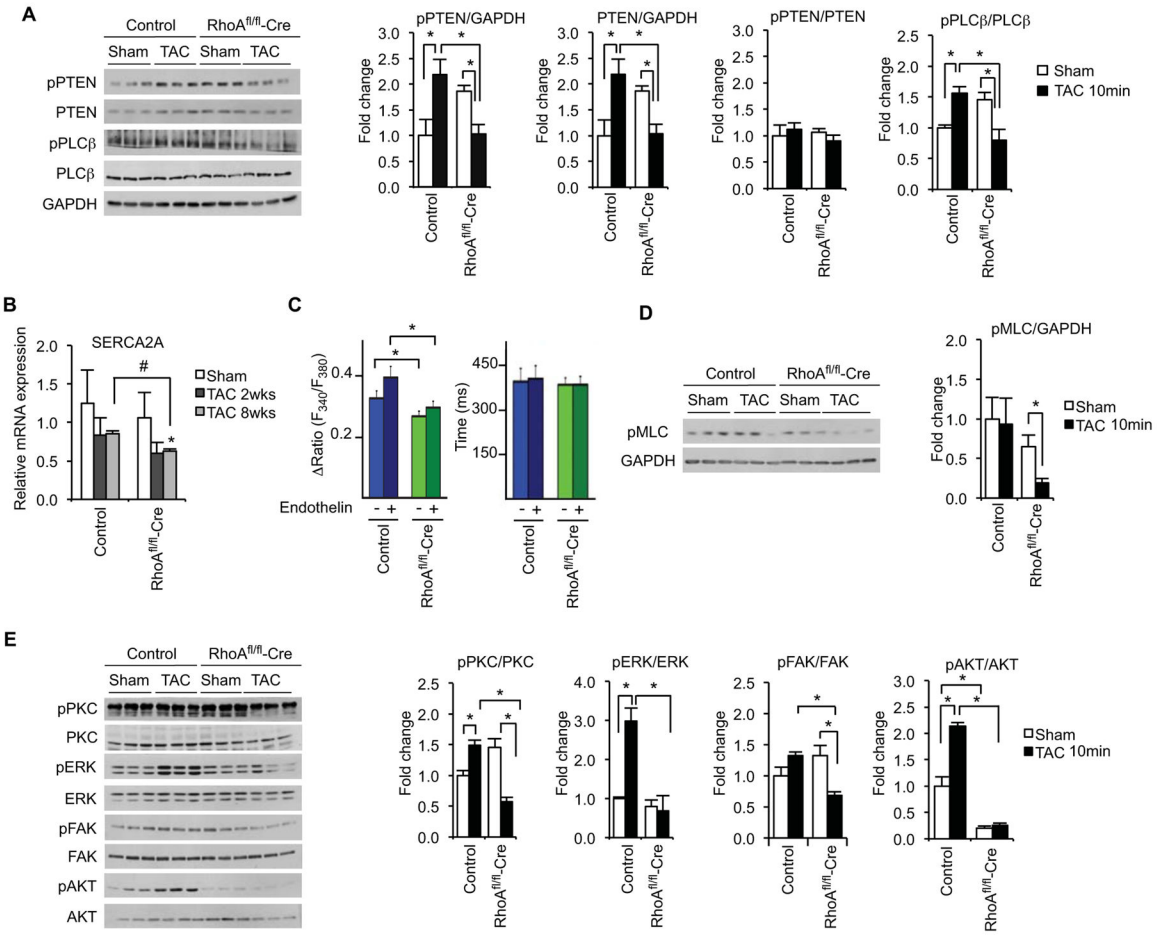

Figure 2. Cardiomyocyte-specific deletion of RhoA may affect contractility by modulating calcium handling and myosin light chain activation and accelerating dilation through aberrant Erk and Akt activities

(A) Whole heart lysates from control or $RhoA^{fl/fl}$-Cre mice subjected to either sham or acute TAC for 10 minutes were immunoblotted for phosphorylated PTEN and PLCβ, with total PTEN, PLCβ, and GAPDH as loading controls. Each lane represents one animal. (B) SERCA2A mRNA expression as assessed by qRT-PCR (n=3–4 mice/group), which was normalized to *RPL13* mRNA. Results were normalized to sham-operated mice of the same genotype. Each sample was assessed in triplicate. (C) Percent change in amplitude of Ca^{2+} transients and time constant of Ca^{2+} decay from the indicated genotypes in the absence or presence of endothelin. At least 3 animals were used for each genotype with a total of 20–25 myocytes under each condition. (D) Whole heart lysates were immunoblotted for phosphorylated myosin light chain (pMLC), with total GAPDH used as the loading control. (E) Whole heart lysates were immunoblotted for phosphorylated PKC, Erk1/2, FAK, and AKT antibodies, with total PKC, Erk1/2, FAK, and AKT used as loading controls. In (D) and (E), n=3 animals per group, and each lane represents one animal. Data in graphs represent mean ± SEM; **p*<0.05, compared to corresponding shams and #*p*<0.05. All p values were derived from ANOVA and Bonferroni post-test when ANOVA was significant.

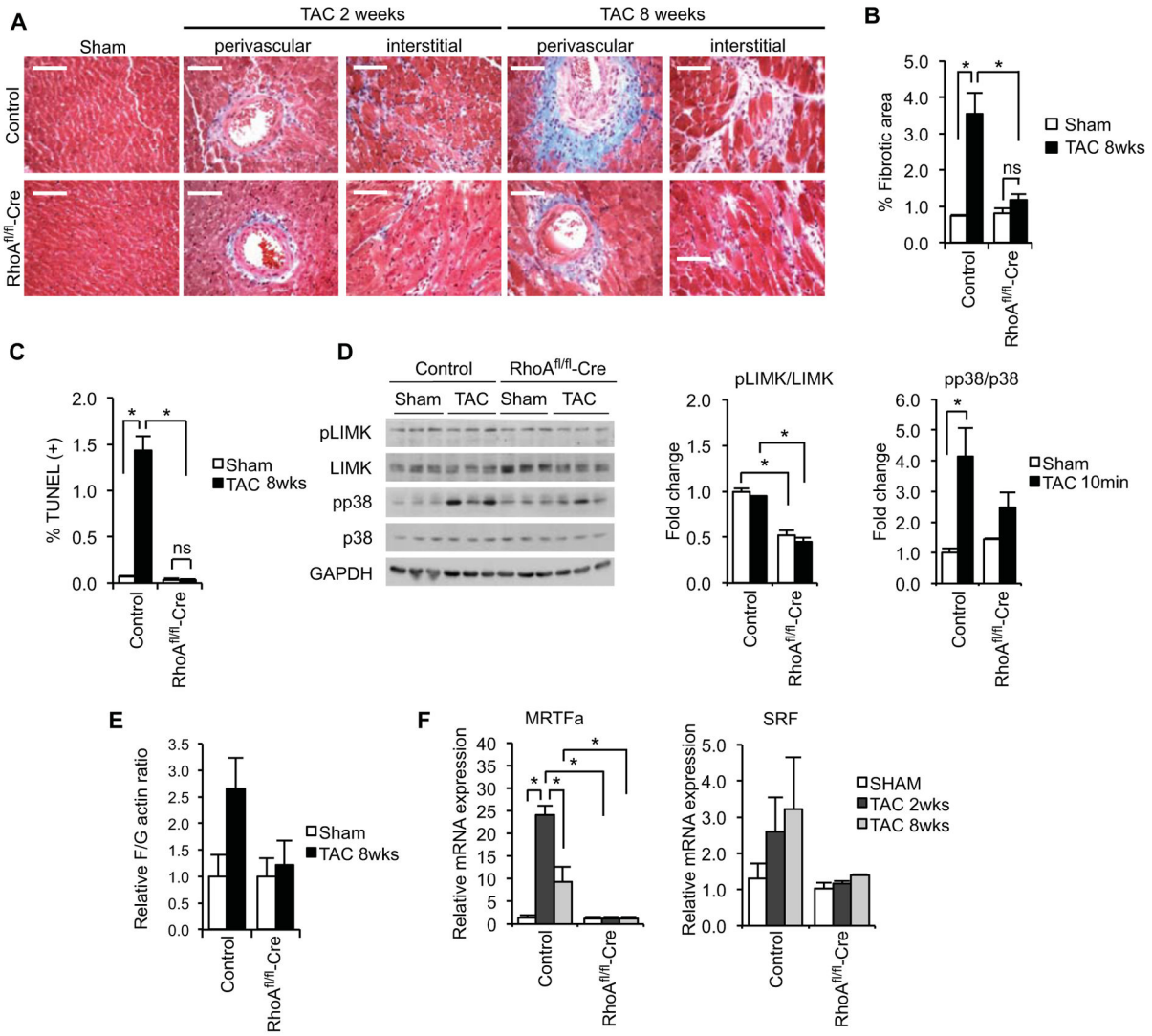

Figure 3. Cardiomyocyte-specific deletion of RhoA reduces cardiac fibrosis induced by pressure overload

(A) Perivascular and interstitial fibrosis in control and RhoA$^{fl/fl}$-Cre mouse hearts following either sham operation or TAC for 2 or 8 weeks, as assessed by Masson-Trichrome staining of paraffin-embedded longitudinal sections. Scale bar, 100 μm. Images are respresentative of n=4 animals/group. **(B)** Quantification of fibrotic area from n=4 animals/group from control or RhoA$^{fl/fl}$-Cre mouse hearts following either sham operation or TAC for 8 weeks. **(C)** Quantification of apoptotic cells (positive for TUNEL staining) from control or RhoA$^{fl/fl}$-Cre mouse hearts following either sham operation or TAC for 8 weeks. N=3 animals per treatment, with at least 5 sections quantified per heart. **(D)** Whole heart lysates from either control or RhoA$^{fl/fl}$-Cre mice subjected to either sham or acute TAC for 10 minutes were immunoblotted for phosphorylated LIMK and p38 MAPK antibodies, with total LIMK, p38, and GAPDH as loading controls. Each lane represents one animal, where n=3 animals/group **(E)** F-Actin to G-Actin ratios of control and RhoAfl/fl-Cre mouse hearts following either sham operation or TAC for 8 weeks. Results were normalized to relative sham-operated

mice. n=3 mice/group. Each sample was assessed in triplicate. Data in graphs represent mean ± SEM. **(F)** *MRTFa* and *SRF* mRNA expression as assessed by qRT-PCR (n=3–4 mice/group), which was normalized to *RPL13* mRNA. Results were normalized to sham-operated mice of the same genotype. Each sample was assessed in triplicate. Data in graphs represent mean ± SEM;*$p<0.05$. All p values were derived from ANOVA and Bonferroni post-test when ANOVA was significant.

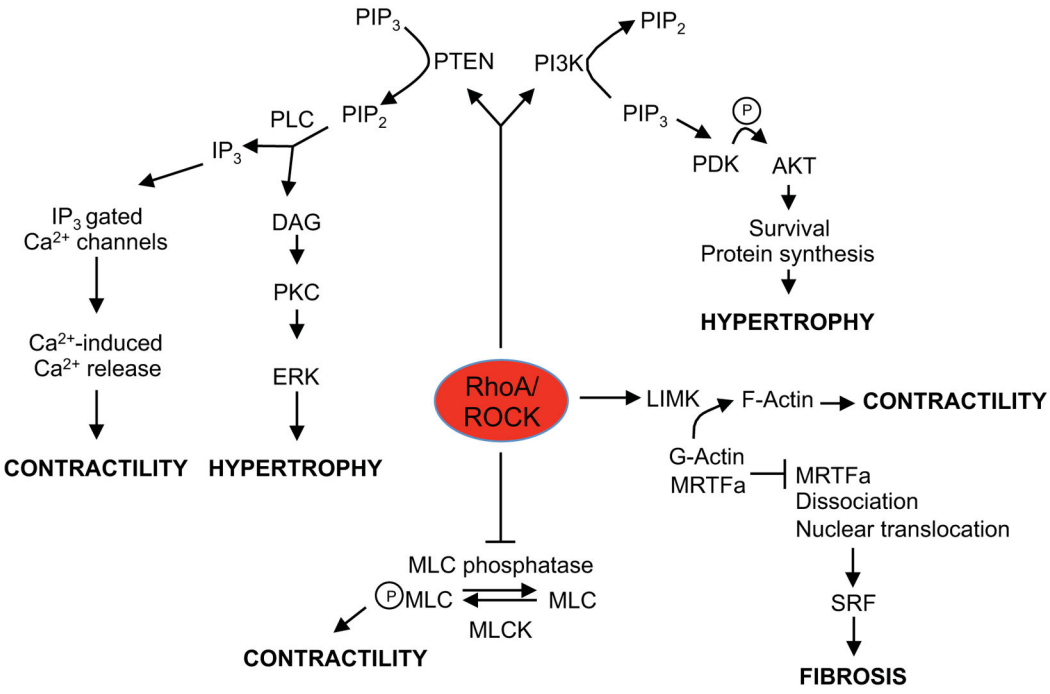

Figure 4. Model for the role of cardiomyocyte-specific expression of RhoA in pathological hypertrophy

RhoA sustains and enhances the compensatory hypertrophic signaling responses to stress in the heart. We propose that RhoA (i) increases contractility through increased calcium and MLC signaling, (ii) sustains hypertrophy through increased activities of both ERK1/2 and AKT, and (iii) initiates the fibrotic response through activation of LIMK, the MAPK p38, and induction of transcriptional regulators of fibrosis.